



OPEN

Divalent magnesium restores cytoskeletal storage lesions in cold-stored platelet concentrates

Konstanze Aurich¹✉, Jan Wesche¹, Martin Ulbricht^{1,3}, Oliver Otto², Andreas Greinacher¹ & Raghavendra Palankar¹

Cold storage of platelet concentrates (PC) has become attractive due to the reduced risk of bacterial proliferation, but in vivo circulation time of cold-stored platelets is reduced. Ca^{2+} release from storage organelles and higher activity of Ca^{2+} pumps at temperatures $< 15^\circ\text{C}$ triggers cytoskeleton changes. This is suppressed by Mg^{2+} addition, avoiding a shift in Ca^{2+} hemostasis and cytoskeletal alterations. We report on the impact of 2–10 mM Mg^{2+} on cytoskeleton alterations of platelets from PC stored at room temperature (RT) or 4°C in additive solution (PAS), 30% plasma. Deformation of platelets was assessed by real-time deformability cytometry (RT-DC), a method for biomechanical cell characterization. Deformation was strongly affected by storage at 4°C and preserved by Mg^{2+} addition ≥ 4 mM Mg^{2+} (mean \pm SD of median deformation 4°C vs. $4^\circ\text{C} + 10$ mM Mg^{2+} 0.073 ± 0.021 vs. 0.118 ± 0.023 , $p < 0.01$; $n = 6$, day 7). These results were confirmed by immunofluorescence microscopy, showing that $\text{Mg}^{2+} \geq 4$ mM prevents 4°C storage induced cytoskeletal structure lesion. Standard in vitro platelet function tests showed minor differences between RT and cold-stored platelets. Hypotonic shock response was not significantly different between RT stored ($56.38 \pm 29.36\%$) and cold-stored platelets with ($55.22 \pm 11.16\%$) or without magnesium ($45.65 \pm 11.59\%$; $p = 0.042$, all $n = 6$, day 1). CD62P expression and platelet aggregation response were similar between RT and 4°C stored platelets, with minor changes in the presence of higher Mg^{2+} concentrations. In conclusion, increasing Mg^{2+} up to 10 mM in PAS counteracts 4°C storage lesions in platelets, maintains platelet cytoskeletal integrity and biomechanical properties comparable to RT stored platelets.

Platelet transfusions are a mainstay of treatment in patients with hypoproliferative thrombocytopenia or major hemorrhage¹. Platelet concentrates are stored at room temperature (RT), which preserves in vivo platelet survival and recovery. However, this increases the risk for bacterial growth. Cold storage of platelet concentrates at 4°C reduces the risk of bacterial proliferation¹. Recent studies have shown that cold storage maintains and even improves some in vitro platelet functions in comparison to storage at RT^{2,3}. However, the in vivo circulation time/life span of cold-stored platelets is considerably reduced^{4,5}. Loss of glycoprotein Iba (GPIba) due to increased metalloproteinase ADAM17 activity and glycan modifications are thought to play a role^{6,7}. Cleavage of terminal sialic acid and clustering of exposed β -N-acetylglucosamines of GPIba⁵ exposes β -galactose on the platelet surface. This is recognized by the Ashwell Morell receptor of hepatocytes or liver macrophages, which then phagocytose platelets^{8,9}. Furthermore, temperatures below 15°C induce divalent calcium (Ca^{2+}) release from platelet storage organelles, and higher activity of Ca^{2+} pumps both results in increased intracellular Ca^{2+} ⁴. This triggers signaling cascades leading to cytoskeleton rearrangements and platelet shape change¹⁰, thought to mainly occur as a result of increased activity of the Ca^{2+} dependent cysteine protease calpain, which cleaves several of the cytoskeletal proteins and protein kinase C¹¹. The Ca^{2+} pump transient receptor potential melastatin-like 7 channel (TRPM7) also regulates magnesium (Mg^{2+}) influx into platelets. Mg^{2+} dependent TRPM7 kinase phosphorylates non-muscle myosin IIA (NMMIIA) that mediates the contractility of the actin cytoskeleton^{12–14}. Mg^{2+} reverses cold-induced intracellular Ca^{2+} increase and inhibits consecutive cytoskeletal alterations¹². Cytoskeletal integrity thus may serve as a sensitive read-out for cold storage induced platelet cytoskeleton lesions. To assess cytoskeleton-dependent biomechanical properties of platelets, several biophysical methods are available¹⁵. We

¹Institut für Transfusionsmedizin, Universitätsmedizin Greifswald, Sauerbruchstraße, 17475 Greifswald, Germany. ²Zentrum Für Innovationskompetenz: Humorale Immunreaktionen Bei Kardiovaskulären Erkrankungen, Universität Greifswald, Fleischmannstr. 42, Greifswald, Germany. ³Present address: Institut Für Pharmazie, Universität Greifswald, Friedrich-Ludwig-Jahn-Straße 17, Greifswald, Germany. ✉email: konstanze.aurich@med.uni-greifswald.de

Cell count	Whole blood before filtration	Whole blood after filtration
Red blood cell ($\times 10^{12}/L$)	5.3 ± 0.3	6.5 ± 2.2
Leukocytes ($\times 10^9/L$)	5.8 ± 1.1	0
Platelets ($\times 10^9/L$)	247.3 ± 34.6	1.9 ± 0.2

Table 1. Cell counts before and after filtration of whole blood by LEUCOFLEX® LXT filter (mean \pm standard deviation, $n = 3$).

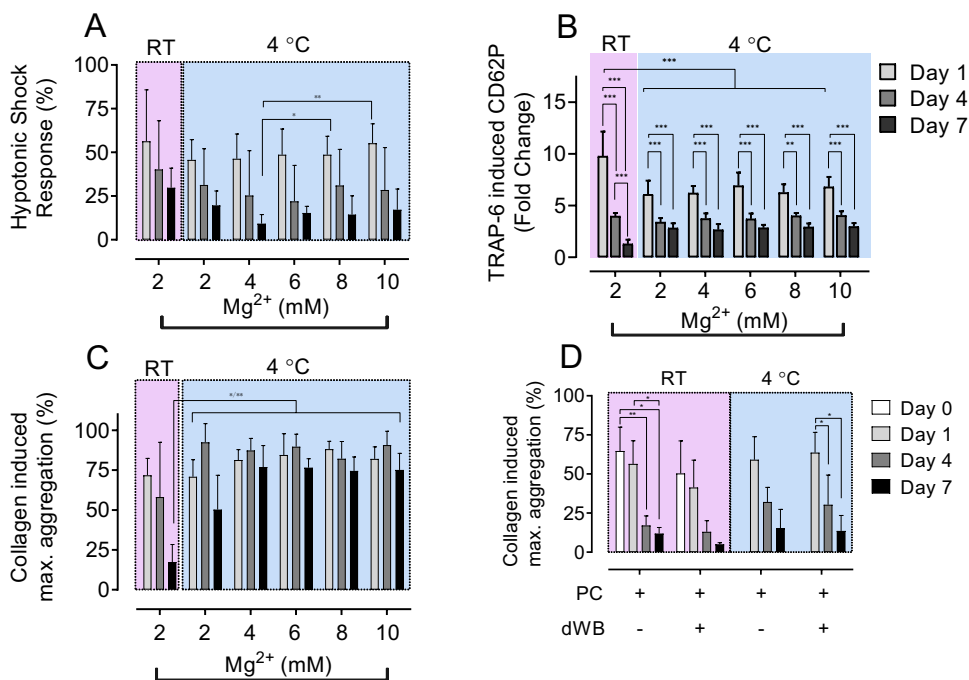


Figure 1. (A) Hypotonic shock response, (B) fold increase of CD62P mean fluorescence intensity after 20 μ M TRAP-6 addition in comparison to buffer-control, and (C) maximum aggregation after 8 μ g/mL collagen I addition to platelets from PC stored at RT + 2 mM Mg^{2+} , 4 $^{\circ}$ C + 2, 4, 6, 8 or 10 mM Mg^{2+} ($n = 6$, mean \pm SD). (D) Maximum aggregation after 8 μ g/mL collagen I addition to platelets from PC stored at RT or 4 $^{\circ}$ C either subsequently added to platelet depleted, tempered whole blood (dWB) or not ($n = 6$, mean \pm SD). PC platelet concentrate, RT room temperature, Mg^{2+} magnesium, SD standard deviation, * $p < 0.05$, ** $p < 0.01$, *** $p < 0.001$. Statistical analysis is performed using one way ANOVA with multiple comparisons.

used real-time deformability cytometry (RT-DC), for mechanical characterization of platelets with high throughput of up to 1,000 cells per second to evaluate the impact of cold storage on platelet cytoskeleton^{16–19}.

Here, we report that the addition of up to 10 mM Mg^{2+} to platelets stored in platelet additive solution (PAS) plus 30% plasma prevents cytoskeleton alterations during long-term cold storage at 4 $^{\circ}$ C, while maintaining platelet function. In addition, we present a new ex vivo quality control approach to assess platelet concentrates in a whole blood matrix.

Results

Leukocyte and platelet depleted whole blood as a matrix to assess the function of platelet concentrates. We developed a method, which allows ex vivo quality control of PC under whole blood conditions. Leukocytes and platelets are considerably reduced by inline filtration of whole blood (Table 1). This provides a near platelet-free whole blood matrix. This platelet-depleted whole blood can be spiked with platelets of interest to assess platelet function in the presence of red cells and plasma proteins.

Magnesium does not adversely affect platelet function in vitro. We prepared PC in 70% PAS-E storage buffer (which contains 2 mM Mg^{2+}) plus 30% plasma and added 2, 4, 6, and 8 mM Mg^{2+} before storage (final Mg^{2+} concentrations 2, 4, 6, 8, 10 mM). The additional magnesium did not exceed the physiological tonicities as it results in a maximum osmolarity of 319 mOsm/L (Supplementary Fig. S1).

Hypotonic shock response did not differ substantially between the different storage conditions or Mg^{2+} concentrations (Fig. 1A). Also, increasing Mg^{2+} concentrations did not alter platelet reactivity to TRAP-6, as measured by CD62P expression, after 4 $^{\circ}$ C storage (Fig. 1B), which was reduced in comparison to RT stored

platelets at day 1: fold change RT (2 mM Mg²⁺) 9.8 ± 2.4 vs. 4 °C (2 mM Mg²⁺) 6.1 ± 1.3 ($p < 0.001$). Thereafter the differences were minor between both storage conditions. Significant differences in CD62P expression occur between storage days 1 and 4 or 7 independently of the storage conditions.

In contrast to TRAP-6, platelet response to collagen (8 µg/mL) was better preserved in cold stored platelets after 7 days of storage (day 7: RT (2 mM Mg²⁺) maximum aggregation 22.54 ± 9.61% vs 4 °C (2 mM Mg²⁺) 45.96 ± 19.24%, $n = 6$, $p < 0.01$), especially at higher magnesium concentrations after 7 days of storage (4 °C + 10 mM Mg²⁺: maximum aggregation 77.97 ± 5.87%, $n = 6$, $p < 0.01$, Fig. 1C).

Spiking leukocyte and platelet depleted whole blood with platelets from differently stored PC and rewarming them at 37 °C for 1 h did not substantially change the aggregation response to collagen compared to platelets measured in PRP (Fig. 1D).

Magnesium prevents platelet cytoskeleton storage lesions. The deformation to area scatterplots by RT-DC showed an apparent decrease in deformation and cell area of platelets stored at 4 °C (Fig. 2A). This was primarily prevented by increasing concentrations of Mg²⁺. For all six PC tested, median deformation ($n \geq 20,000$ single platelets) decreased due to storage at 4 °C and generally increased with Mg²⁺ addition (Fig. 2B). This effect was particularly pronounced on storage day 7.

Next, we assessed the integrity and reorganization of the marginal band tubulin ring. After storage at RT the tubulin ring is visible, both in the microscopic image and by the separated peaks of the cross-sectional fluorescence signals (Fig. 3A). Storing platelets at 4 °C induces disorganization of tubulin and distribution of the fluorescence signal throughout the cell (Fig. 3A bottom, Fig. 3B top left). Rewarming of platelets from cold-stored PCs in platelet-depleted whole blood has no consequences on the disorganization of the tubulin ring at 4 °C (Fig. 3B top right). Additional Mg²⁺ prevented tubulin depolymerization with the, most substantial effects at 8 and 10 mM Mg²⁺ (Fig. 3B bottom).

Magnesium addition does not impair desialylation of platelets during cold storage. Cold storage initialized desialylation of platelet surface, resulting in increased phagocytosis of platelets by hepatocytes via the Ashwell-Morell receptor. We determined the binding of two different lectins, *Erythrina cristagalli* lectin (ECL) and *Ricinus communis* lectin agglutinin (RCA), to desialylated galactose and β-N-acetyl glucosamine (GlcNAc) residues on the surface of RT and cold-stored platelets with or without additional magnesium. Lectin binding is reduced due to cold storage but did not change with increasing magnesium concentration (Fig. 4).

Discussion

In this study, we provide evidence that increasing the Mg²⁺ concentration of the storage medium up to 10 mM prevents platelet cytoskeleton storage lesions during storage at 4 °C. Otherwise, platelets storage at 4 °C leads to shape change, spherocytosis, and decreased mean platelet volume^{4,10}. Recently, it has been shown that the platelet shape change, which is driven by the cytoskeleton, is mainly caused by two processes: (i) increased activity of calpain, a Ca²⁺ dependent cysteine protease, which cleaves platelet actin leading to rigid, stiff cells²⁰ and (ii) upregulated NMMIIA activity, a motor protein mediating contractility of the platelet actin cytoskeleton¹². During cold storage, intracellular Ca²⁺ increases due to active transport or passive Ca²⁺ leakage from platelet organelles and reduced Ca²⁺ pump activity leading to a slow accumulation of Ca²⁺¹⁰. Subsequently, store-operated Ca²⁺ entry (SOCE) and receptor-operated Ca²⁺ entry regulate further Ca²⁺ increase, which regulates platelet integrin αIIbβ3 activation by calpain and platelet degranulation^{11,21,22}. TRPM7 channel is the key channel controlling Mg²⁺ and Ca²⁺ exchange in platelets¹². TRPM 7 kinase activity is mediated by Mg²⁺ and directly affects intracellular Ca²⁺ concentration via SOCE, phospholipase C and γ²¹³. As a consequence Mg²⁺ supplementation counteracts intracellular Ca²⁺ increase, which prevents calpain activation. Furthermore, NMMIIA activity can be inhibited by enhanced intracellular Mg²⁺ concentrations, which increases adenine diphosphate (ADP) release, followed by induction of NMMIIA C-terminus phosphorylation²⁰. This interplay between Ca²⁺ and Mg²⁺ is key to our concept to prevent alterations of the platelet cytoskeleton during cold storage by Mg²⁺ supplementation.

We also demonstrate that cold-induced cytoskeletal disorganization of platelets during storage at 4 °C is prevented by the addition of Mg²⁺ into the storage media. This we show by two independent methods: First by confocal laser scanning microscopy of platelet cytoskeletal proteins. However, immunofluorescence studies of platelets are low throughput and are at risk of a selection bias. Second by RT-DC, which we have recently introduced as a high throughput method to assess platelet biomechanics²³. RT-DC allows measuring thousands of platelets within minutes and is the first method providing an unbiased, comprehensive analysis of the biomechanics of platelets in platelet concentrates. Consistent with our immunofluorescent studies, RT-DC shows preservation of platelet deformation at 4 °C by the addition of Mg²⁺.

The main reason for the reduced platelet survival after cold storage might be desialylation of platelet glycoproteins resulting in increased phagocytosis by hepatocytes. We showed that increased Mg²⁺ addition does not reduce desialylation during cold storage of platelets in vitro. It is more likely that magnesium affects platelet survival by other mechanisms. The exact molecular mechanisms of how increased Mg²⁺ concentrations prevent changes of the platelet cytoskeleton are still only partly understood. One proposed mechanism is by inhibiting the cold-induced increase in intracellular Ca²⁺ concentrations without activating calpain. Another potential mechanism might be the reduction of intracellular Ca²⁺ release after activation of GPIIb. The binding of von Willebrand factor (vWF) to a mechanosensitive domain of GP Iba triggers outside-in mechanotransduction signals in platelets, leading to intracellular Ca²⁺ release²⁴. Platelet concentrates have to be stored under agitation that platelets can move along the gas permeable plastic membrane of the storage bag. This allows the release of CO₂ and uptake of O₂. Likely the shear stress on the plastic membrane of the platelet concentrate storage bag unfolds vWF, which then binds GPIIb mediating mechano-signaling, which finally leads to an increase in

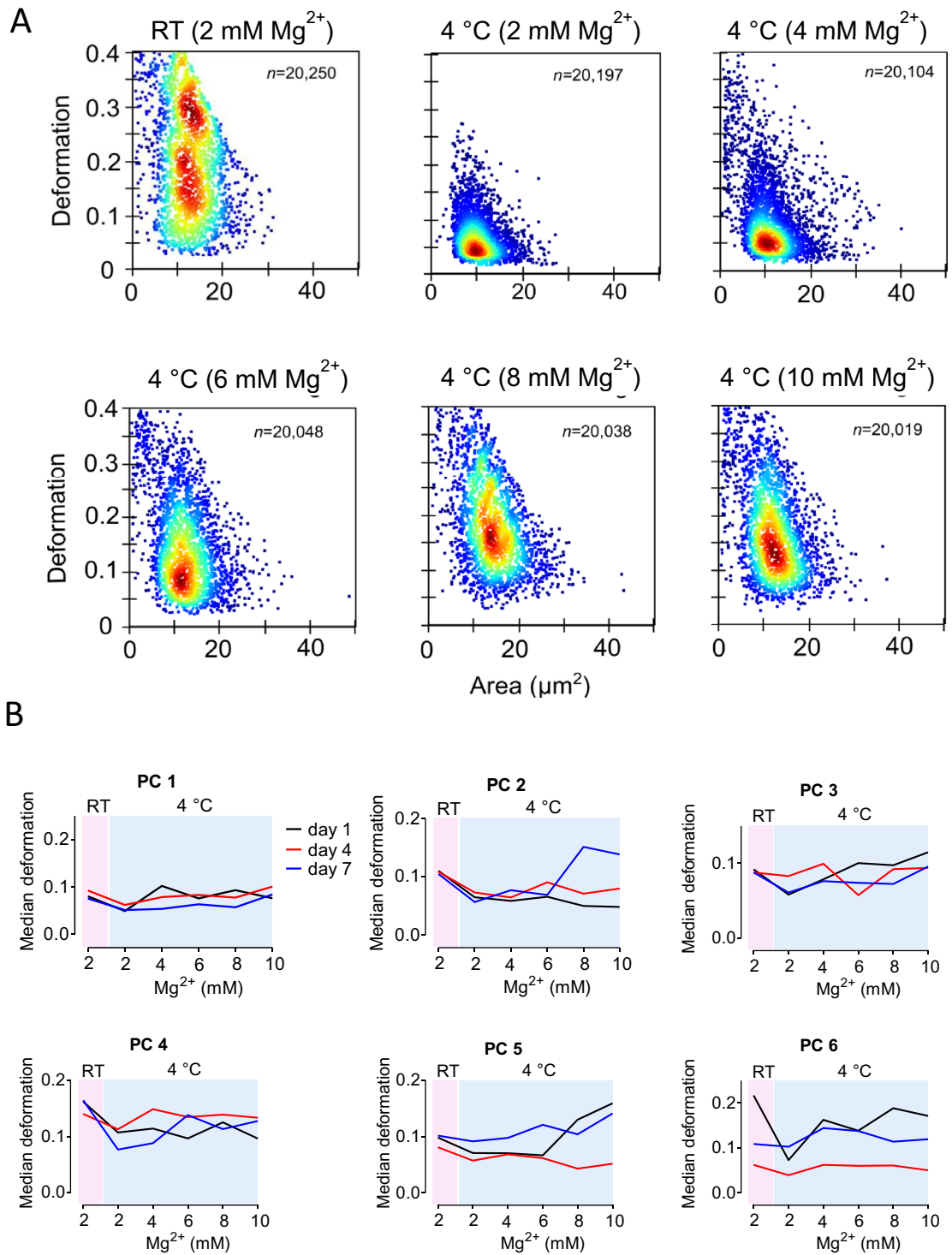


Figure 2. (A) Deformation vs cell area scatterplots determined by RT-DC of platelets from one PC stored for 7 days under different conditions at RT + 2 mM Mg^{2+} , 4 °C + 2, 4, 6, 8 or 10 mM Mg^{2+} . (B) Median deformation of platelets in platelet concentrates (PC, $n=6$) for each magnesium concentration and storage temperature are given for day 1 (black), day 4 (red) and day 7 (blue), $n \geq 20,000$ platelets. RT room temperature, Mg^{2+} magnesium.

plasmatic Ca^{2+} concentrations. In line with this hypothesis, blocking the vWF-GPIIb interaction by the peptide OS1 that blocks vWF binding to GPIIb, resulted in increased post-transfusion recovery and survival of cold-stored platelets in mice²⁵.

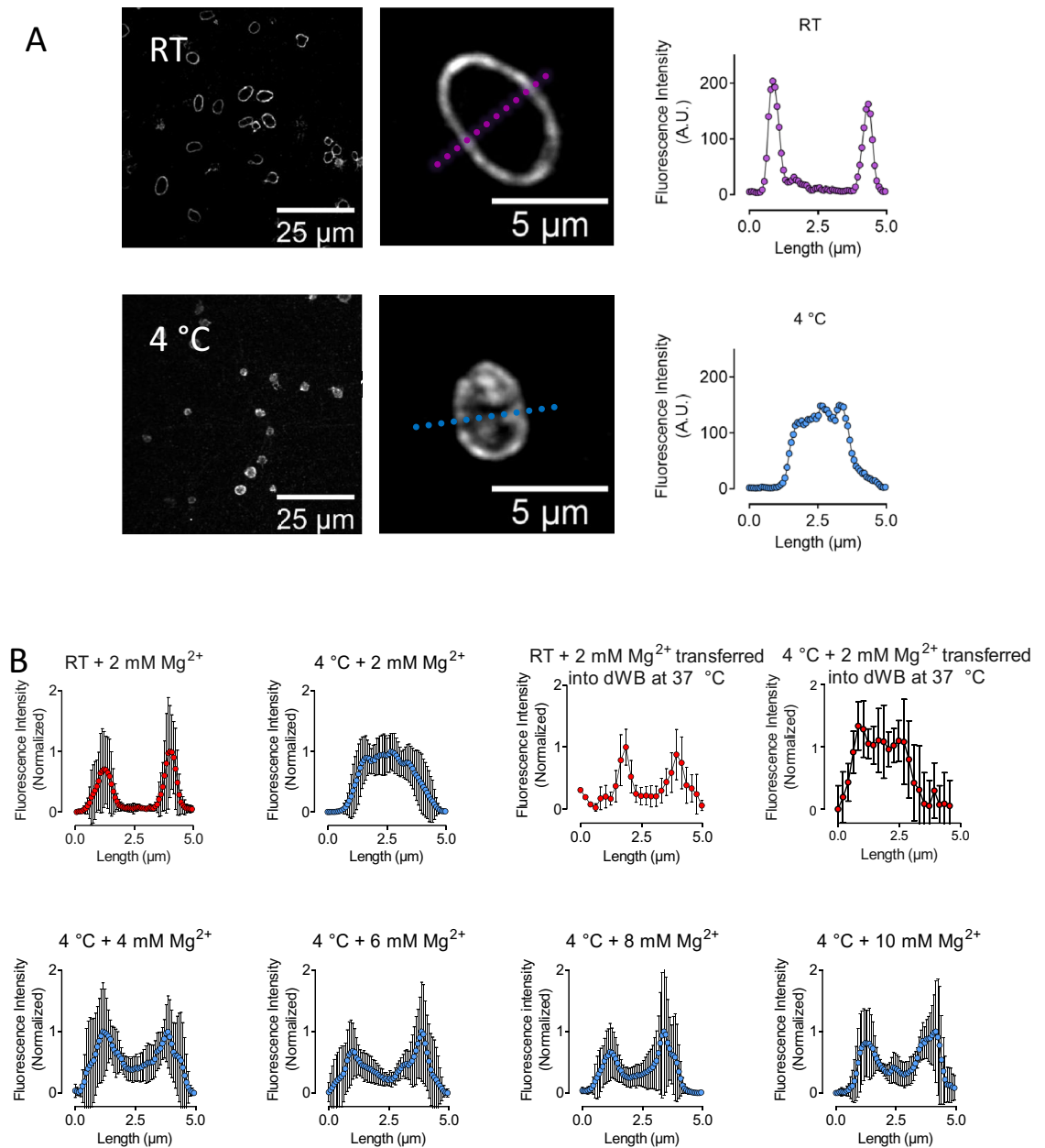


Figure 3. (A) Fluorescence image and intensity of stained α -tubulin along an axis of the cross-section of platelets from PC stored at RT or 4 $^{\circ}\text{C}$. (B) Normalized fluorescence intensity of stained α -tubulin along an axis of the cross-section of platelets stored for 24 h under different conditions ($n = 10$, mean \pm standard deviation). α -tubulin was stained by mouse anti-human α -tubulin IgG + secondary donkey anti-mouse IgG Alexa Flour 568. RT room temperature, Mg^{2+} magnesium, dWB platelet depleted whole blood.

The currently used PAS-E already contains 2 mM Mg^{2+} . However, this concentration is not sufficient to prevent platelet storage lesions of the cytoskeleton. Our study shows that at least Mg^{2+} concentrations of 4 mM are required to prevent platelet cytoskeleton storage lesions. Increasing ion concentrations raise the issue of changing the osmolarity of the storage solution. However, at 10 mM Mg^{2+} PAS, osmolarity increased only by 4%, which is obviously well tolerated by platelets.

These concentrations are safe for the transfusion recipient. Mg^{2+} had been used extensively in obstetrics to control uterus contractions in concentrations up to 100 mmol given intravenously. This is 40-fold more than the Mg^{2+} dose given with a standard platelet concentrate²⁶. Even the high concentrations given in obstetric patients have shown to be safe regarding the cardiovascular system and liver disease^{27–29}.

Mg^{2+} addition to platelet storage buffers has also been tested by others. Storing platelets in PAS containing up to 6 mM Mg^{2+} resulted in relatively minor changes in platelet metabolism (platelet count, pH, lactate concentration)³⁰. Storage of platelets in PAS containing up to 2 mM Mg^{2+} resulted in higher platelet quality and reduced

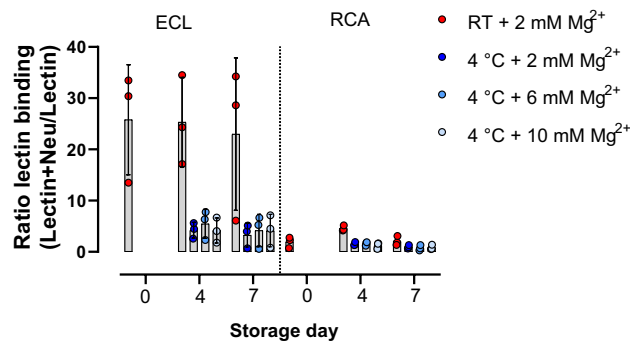


Figure 4. Impact of Mg²⁺ addition to desialylation of platelets. Binding of fluorescently labeled *Erythrina cristagalli* lectin (ECL) and *Ricinus communis* agglutinin (RCA) to platelet surface glycoproteins of RT and cold-stored platelets with or without Mg²⁺ in the presence and absence of sialidase during 7 days storage. RT room temperature, Mg²⁺ magnesium. n = 3, mean + standard deviation.

cytokine release in vitro^{31,32}. A storage medium containing adenine, lidocaine, and 7 mM Mg²⁺ in PAS or plasma stored platelets preserved the aggregation response to ADP and TRAP-6 at RT and 4 °C storage³³. In agreement with these findings, we observed that the aggregation response of platelets to collagen in PAS + with 30% plasma was better preserved during storage of 7 days at 4 °C in the presence of increasing concentrations of Mg²⁺.

Recently, we observed that cold storage also triggers phosphatidylserine exposure indicating platelet apoptosis². Interestingly, Getz et al. observed that platelet apoptosis is reduced in citrate-free PAS³⁴. Our results suggest that this might be due to increasing available Mg²⁺ by the absence of chelating agent citrate.

Cold storage of platelets also triggers an increased activation of metalloproteinases such as ADAMTS17, which in turn cleaves sialic acid from and GPIb leading to enhanced recognition and clearance of platelets by hepatic macrophages. ADAMTS17 inhibitors such as GM6001 block this effect in vitro³⁵. During platelet storage also caspase enzymes are expressed and activated. They cleave numerous cellular proteins leading to cell death. Accordingly, it has been shown that Caspase-3 inhibitors block apoptosis during storage³⁶.

In view of these other effects of cold storage induced platelet lesions, likely a combination of different approaches is required to preserve platelet in vivo recovery, survival, and function after cold storage of platelet concentrates.

Here we have shown that increasing Mg²⁺ concentrations to up to 10 mM is one important and easy to apply approach towards preventing cold-induced cytoskeleton storage lesions in platelets.

Methods

Platelet concentrates. Whole blood was collected from healthy donors according to the German guidelines for hemotherapy with written informed consent. The study was approved by the ethical board of the Universitätsmedizin Greifswald, Germany. All methods used were performed in accordance with the relevant guidelines and regulations. Pooled platelet concentrates from whole blood buffy coats were produced according to the standard method for producing therapeutic platelet concentrates. In brief, after centrifugation (4000×g, 10 min), whole blood in citrate phosphate dextrose solution (CPD, Macopharma, France) was separated into red cell concentrate, plasma, and buffy coat. Buffy coats of 4 blood group identical donations were pooled, and 250 mL additive solution PAS-E (SSP +, Macopharma) was added. PAS-E itself contains 2 mM magnesium. By centrifugation (720 g, 15 min), platelets were separated from residual red blood cells and leukocyte depleted (LEUCOFLEX® LXT Filter, Macopharma). PC bags were split into six bags (gas permeable bags, Macopharma) and stored under agitation at RT or 4 °C for 7 days.

Platelet concentrate storage. Magnesium sulfate solution (Inresa Arzneimittel GmbH, Germany) was added to four of the six bags in increasing concentrations. 0, 2, 4, 6, 8 mM (final concentrations: 2, 4, 6, 8, 10 mM). PC was stored under agitation on an orbital shaker (LPR1, Melco Engineering Corp., USA). Sampling took place on day 0 (production day), day 1, day 4 and day 7.

In vitro platelet function testing. The ability of platelets to respond to a hypotonic environment was determined as hypotonic shock response (HSR) by light transmission aggregometry (LTA)³⁷. Platelets were exposed to distilled water or 0.9% w/v sodium chloride solution as a control. Due to the osmotic gradient, the water diffuses into the platelets, which leads to their swelling. As a result of swelling, the refractive index of platelets increases, resulting in a decrease in light transmission. The percentage of HSR was calculated as (T2 – T3)/(T2 – T1) × 100, with T1 = transmission of platelet suspension in sodium chloride; T2 = transmission of platelets in distilled water; T3 = “plateau” transmission value after 4 min of platelets incubated in distilled water.

Platelet activation was determined by CD62P expression before and after the addition of thrombin receptor activating peptide 6 (TRAP-6). 3 × 10⁸/mL platelets were incubated for 15 min at 37 °C with 20 μM TRAP-6 (Hart Biologicals, UK) or PBS buffer (w/o Ca²⁺, Mg²⁺, pH 7.2) as the negative control, fixed 20 min with 0.5% paraformaldehyde (Morphisto Laborchemikalien, Germany) and washed twice (2 mL PBS; 650 g, 7 min, RT). The pellet was resuspended in 500 μL PBS and analyzed by flow cytometry (FC500, Beckman Coulter, USA).

Platelets were gated using a mouse-anti-human CD41-PeCy5 (clone P2, Beckman Coulter) labeled monoclonal antibody. The increase of CD62P exposure on CD41-positive events was determined using CD62P-FITC (clone CLBThromb/6, Beckman Coulter, USA). The mean fluorescence intensity of TRAP-6 activated platelets is given as fold increase in comparison to the respective buffer controls.

Platelet aggregation was analyzed over 7 min at 37 °C in a 4-channel-aggregometer (DiaSys, Germany) after the addition of 8 µg/mL collagen (Mölab, Germany).

For all in vitro platelet function analyzes we analyzed six pooled PC, in summary platelets from n = 24 different donors.

Whole blood as a matrix for ex vivo quality control of platelet concentrates. To simulate in vivo conditions, we prepared platelet-depleted whole blood (dWB). Whole blood was collected from a healthy donor blood group O according to the German guidelines for hemotherapy, using a bag system containing citrate-phosphate-derivative with adenine (CPDA) solution for anticoagulation. Directly after donation, whole blood was leukocyte and platelet depleted by a LEUCOFLEX® LXT leukocyte depletion filter, which removes 99.999% of leukocytes and platelets (Macopharma, France). Cell counts were determined before and after filtration by an automated blood cell analyzer (Sysmex XP300, Sysmex Deutschland GmbH, Germany). Depleted whole blood was stored at 4 °C until use. Platelets stored at 4 °C at different Mg²⁺ concentrations were either analyzed directly in platelet storage buffer PAS-E or spiked into depleted whole blood to achieve a final platelet concentration of 300,000/µL and rewarmed at 37 °C for 1 h before analyses. For aggregometry studies, whole blood was centrifuged at 120×g for 20 min to obtain PRP.

Biomechanical platelet characterization. RT-DC is a method for the biomechanical characterization of cells with throughput rates of up to 1,000 per second (Supplementary Fig. S2)²³. In brief, platelets are pumped at flow rates of 0.006 µL/s from a reservoir through a narrow channel on a chip assembled on the AcCellerator system (Zellmechanik Dresden). The microfluidic chip consists of a constriction of 15 µm × 15 µm cross-section with a length of 300 µm and is connected to a syringe pump (NemeSys, Cetoni, Germany). Upon entering the channel and during the passage, the cells are subjected to both hydrodynamic shear forces and different pressure gradients. The deformation of platelets caused by these external forces are recorded by a high-speed camera. The individual images are then analyzed with an evaluation algorithm (ShapeOut, version 0.8.6, Zellmechanik Dresden) for the deformation of the individual platelet (Supplementary Fig. S2)¹⁷. Samples of n = 6 pooled PC were taken on days 1, 4, and 7 after PC production. For RT-DC 50 µL of platelets in PAS-E/plasma were diluted in Carrier B (Zellmechanik Dresden; 0.6% (w/v) methylcellulose in PBS, without Ca²⁺ and Mg²⁺) to a final concentration of approximately 1 × 10⁷/mL. Calculations are performed at different flow rates representing different experimental conditions.

Analysis of cytoskeleton proteins by immunofluorescence microscopy. Platelets from PC of all 6 storage conditions were adjusted to a platelet count of 50,000 platelets/µL each with 2% paraformaldehyde in PBS (w/o Ca²⁺, Mg²⁺, pH 7.2) and incubated for 15 min at RT. At the end of the incubation period, 100 µL of each sample was cytospin centrifuged by for 5 min at 700 rpm on microscopic slides. Following centrifugation, the slides were washed three times for 5 min at RT with PBS (w/o Ca²⁺, Mg²⁺, pH 7.2) and stored at -20 °C. The cells were treated with permeability buffer (0.1% Triton-X in PBS and BSA 2%) for 10 min at RT in a humid chamber, and cells were then washed twice with 50 µL PBS for 10 min at RT. Platelets were stained for α-tubulin (mouse anti-human α-tubulin IgG, Sigma-Aldrich, St. Louis, Missouri, USA) at RT for at least 1 h, washed again twice with 50 µL PBS and then incubated with 50 µL secondary donkey anti-mouse IgG Alexa Fluor 568 (Abcam, Cambridge, UK) for 1 h at RT, incubated with 50 µL of phalloidin ATTO 488 solution (1:200; ATTO-TEC GmbH, Siegen, Germany) for further 30 min at RT in the dark and then washed twice with PBS. Fluorescence microscopy was performed on a Leica SP5 confocal laser scanning microscope (Leica Microsystems, Wetzlar, Germany) equipped with HCX PL APO lambda blue 40.0x/1.25 OIL UV objective. For image acquisition, fluorescent tags Atto-488 and AlexaFluor-568 were excited by argon (488 nm) and helium-neon (HeNe) 563 nm laser lines, respectively, selected with an acousto-optic tunable filter (AOTF). Fluorescence emission for Atto-488 and AlexaFluor-568 was collected between 505–515 nm and 550–570 nm on hybrid detectors (HyD) and photomultiplier tubes (PMTs), respectively. Assessment of distribution and organization of marginal band α-tubulin staining was performed by measuring cross-sectional line profile (5 µm length and 1 µm width) of non-saturated grayscale fluorescence intensities (pixel values) of immunofluorescent probes across individual platelets in confocal images using Leica Application Suite X (Version 3.7.1, Leica Microsystems, Wetzlar, Germany). Data were plotted using GraphPad Prism version 8.0.0 for Windows, (GraphPad Software, San Diego, California USA). For each storage condition, the microscopic images of at least 10 single platelets were analyzed. In addition, whole blood spiked with platelets from stored PC was also used to prepare blood smears, which were stained as described above. Here, an Olympus BX 40 microscope with UPlanSApo 60x/1.35 Oil objective was used with software cellSensStandard (Imaging Software cellSens, Olympus Corporation, Tokyo, Japan).

Desialylation of stored platelets. To evaluate the effect of Mg addition on desialylation of platelets during storage at 4 °C we determined the binding of fluorescein isothiocyanate (FITC) labeled *Erythrina cristagalli* lectin (ECL) and *Ricinus communis* lectin agglutinin (RCA) to platelet surface glycoproteins of RT and cold stored platelets (n = 3 pooled PC) with or without Mg²⁺ addition. PC was adjusted to a cell count of 300,000/µL and labeled by CD61-AlexaFluore647 platelet marker (Biolegend, USA). FITC labeled RCA and ECL were added (1 µL 1:500 RCA or 1:250 ECL in PAS-E, Biozol, USA) and incubated in the dark for 20 min. After that 200 µL PAS-E was added, and the samples were washed (650×g, 7 min). The binding of ECL and RCA was analyzed

using an FC500 flow cytometer (Beckman Coulter, USA). As a positive control, sialidase (neuraminidase, Sigma Aldrich, USA) was used.

Statistical data evaluation. For all statistical data evaluation we used Graphpad Prism 8.0.1. Statistical significances were calculated by One-Way Analysis of Variance (ANOVA) with multiple comparisons test.

Data availability

The datasets generated during and/or analysed during the current study are available from the corresponding author on reasonable request. All data generated or analysed during this study are included in this published article (and its Supplementary Information files).

Received: 30 June 2021; Accepted: 4 April 2022

Published online: 14 April 2022

References

1. Getz, T. M. Physiology of cold-stored platelets. *Transfus. Apher. Sci.* **58**, 12–15 (2019).
2. Marini, I. *et al.* Cold storage of platelets in additive solution: The impact of residual plasma in apheresis platelet concentrates. *Haematologica* **104**, 207–214 (2019).
3. Wood, B., Padula, M. P., Marks, D. C. & Johnson, L. Refrigerated storage of platelets initiates changes in platelet surface marker expression and localization of intracellular proteins. *Transfusion* **56**, 2548–2559 (2016).
4. Hoffmeister, K. M. *et al.* The clearance mechanism of chilled blood platelets. *Cell* **112**, 87–97 (2003).
5. Rumjantseva, V. & Hoffmeister, K. M. Novel and unexpected clearance mechanisms for cold platelets. *Transfus. Apher. Sci.* **42**, 63–70 (2010).
6. Bode, A. P. & Knupp, C. L. Effect of cold storage on platelet glycoprotein Ib and vesiculation. *Transfusion* **34**, 690–696 (1994).
7. Bergmeier, W. *et al.* Metalloproteinase inhibitors improve the recovery and hemostatic function of in vitro-aged or -injured mouse platelets. *Blood* **102**, 4229–4235 (2003).
8. Li, Y. *et al.* Sialylation on O-glycans protects platelets from clearance by liver Kupffer cells. *Proc. Natl. Acad. Sci. U.S.A.* **114**, 8360–8365 (2017).
9. Sorensen, A. L. *et al.* Role of sialic acid for platelet life span: Exposure of beta-galactose results in the rapid clearance of platelets from the circulation by asialoglycoprotein receptor-expressing liver macrophages and hepatocytes. *Blood* **114**, 1645–1654 (2009).
10. Oliver, A. E., Tablin, F., Walker, N. J. & Crowe, J. H. The internal calcium concentration of human platelets increases during chilling. *Biochem. Biophys. Acta* **1416**, 349–360 (1999).
11. Kuchay, S. M. & Chishti, A. H. Calcipain-mediated regulation of platelet signaling pathways. *Curr. Opin. Hematol.* **14**, 249–254 (2007).
12. Stritt, S. *et al.* Defects in TRPM7 channel function deregulate thrombopoiesis through altered cellular Mg(2+) homeostasis and cytoskeletal architecture. *Nat. Commun.* **7**, 11097 (2016).
13. Gotru, S. K. *et al.* TRPM7 kinase controls calcium responses in arterial thrombosis and stroke in mice. *Arterioscler. Thromb. Vasc. Biol.* **38**, 344–352 (2018).
14. Ngo, A. T. P., McCarty, O. J. T. & Aslan, J. E. TRPM7 (Transient Receptor Potential Melastatin-Like 7) modulates calcium mobilization and platelet function via phospholipase C interactions. *Arterioscler. Thromb. Vasc. Biol.* **38**, 285–286 (2018).
15. Sachs, L., Denker, C., Greinacher, A. & Palankar, R. Quantifying single-platelet biomechanics: An outsider's guide to biophysical methods and recent advances. *Res. Pract. Thromb. Haemost.* **4**, 386–401 (2020).
16. Guzniczak, E. *et al.* High-throughput assessment of mechanical properties of stem cell derived red blood cells, toward cellular downstream processing. *Sci. Rep.* **7**, 14457 (2017).
17. Otto, O. *et al.* Real-time deformability cytometry: On-the-fly cell mechanical phenotyping. *Nat. Methods* **12**, 199–202 (2015).
18. Toepfner, N., Herold, C., Otto, O. & Rosendahl, P. Detection of human disease conditions by single-cell morpho-rheological phenotyping of blood. *Elife* **7**, e29213 (2018).
19. Xavier, M. *et al.* Mechanical phenotyping of primary human skeletal stem cells in heterogeneous populations by real-time deformability cytometry. *Integr. Boil.* **8**, 616–623 (2016).
20. Swenson, A. M. *et al.* Magnesium modulates actin binding and ADP release in myosin motors. *J. Biol. Chem.* **289**, 23977–23991 (2014).
21. Braun, A., Vogtle, T., Varga-Szabo, D. & Nieswandt, B. STIM and Orai in hemostasis and thrombosis. *Front. Biosci.* **16**, 2144–2160 (2011).
22. Varga-Szabo, D., Braun, A. & Nieswandt, B. Calcium signaling in platelets. *J. Thromb. Haemost.* **7**, 1057–1066 (2009).
23. Aurich, K. *et al.* Label-free on chip quality assessment of cellular blood products using real-time deformability cytometry. *Lab Chip* **20**, 2306–2316 (2020).
24. Hansen, C. E., Qiu, Y., McCarty, O. J. T. & Lam, W. A. Platelet mechanotransduction. *Annu. Rev. Biomed. Eng.* **20**, 253–275 (2018).
25. Chen, W. *et al.* Refrigeration-induced binding of von willebrand factor facilitates fast clearance of refrigerated platelets. *Arterioscler. Thromb. Vasc. Biol.* **37**, 2271–2279 (2017).
26. Bachnas, M. A., Akbar, M. I. A., Dachlan, E. G. & Dekker, G. The role of magnesium sulfate (MgSO₄) in fetal neuroprotection. *J. Maternal-Fetal Neonatal Med.* **34**, 966–978 (2019).
27. Tangvoraphonkchai, K. & Davenport, A. Magnesium and cardiovascular disease. *Adv. Chronic Kidney Dis.* **25**, 251–260 (2018).
28. Marques, B. *et al.* Effects of oral magnesium supplementation on vascular function: A systematic review and meta-analysis of randomized controlled trials. *High Blood Pressure Cardiovasc. Prev.* **27**, 19–28 (2019).
29. Liu, M., Yang, H. & Mao, Y. Magnesium and liver disease. *Ann. Transl. Med.* **7**, 578 (2019).
30. Meledeo, M. A., Campbell, J. E., Rodriguez, A. C., Valenciana, M. V. & Cap, A. P. Both acute delivery of and storage with magnesium sulfate promote cold-stored platelet aggregation and coagulation function. *J. Trauma Acute Care Surg.* **79**, S139–145 (2015).
31. Diedrich, B. *et al.* In vitro and in vivo effects of potassium and magnesium on storage up to 7 days of apheresis platelet concentrates in platelet additive solution. *Vox Sang.* **94**, 96–102 (2008).
32. Shanwell, A., Falker, C. & Gulliksson, H. Storage of platelets in additive solutions: The effects of magnesium and potassium on the release of RANTES, beta-thromboglobulin, platelet factor 4 and interleukin-7, during storage. *Vox Sang.* **85**, 206–212 (2003).
33. Bynum, J. A. *et al.* Evaluation of adenosine, lidocaine, and magnesium for enhancement of platelet function during storage. *J. Trauma Acute Care Surg.* **83**, S9–s15 (2017).
34. Getz, T. M., Turgeon, A. & Wagner, S. J. Sodium citrate contributes to the platelet storage lesion. *Transfusion* **59**, 2103–2112 (2019).
35. Jansen, A. J. *et al.* Desialylation accelerates platelet clearance after refrigeration and initiates GPIIb/IIIa metalloproteinase-mediated cleavage in mice. *Blood* **119**, 1263–1273 (2012).

36. Shiri, R., Yari, F., Ahmadinejad, M., Vaeli, S. & Tabatabaei, M. R. The caspase-3 inhibitor (peptide Z-DEVD-FMK) affects the survival and function of platelets in platelet concentrate during storage. *Blood Res.* **49**, 49–53 (2014).
37. Rock, G. & Figueredo, A. Metabolic changes during platelet storage. *Transfusion* **16**, 571–579 (1976).

Acknowledgements

We thank Doreen Biedenweg, Jessica Fuhrmann and Julia Klauke for excellent technical support. OO gratefully acknowledges support from the German Ministry of Education and Research (ZIK grant to OO under grant agreement: 03Z22CN11) and from the German Centre of Cardiovascular Research (Postdoc Start-up Grant to OO under grant agreement: 81X3400107). Funded by the Deutsche Forschungsgemeinschaft (DFG, German Research Foundation)—Project number 374031971—TRR 240 to OO and RP.

Author contributions

K.A. and A.G. conceived the project, developed the experimental setup, and wrote the manuscript. K.A. and O.O. designed and performed all RT-DC experiments. R.P. designed and performed the fluorescence microscopy experiments and wrote the manuscript. J.W., M.U. and K.A. achieved the platelet concentrate experiments. All authors contributed to editing and revision the manuscript.

Funding

Open Access funding enabled and organized by Projekt DEAL.

Competing interests

OO is co-founder of Zellmechanik Dresden GmbH, distributing real-time deformability cytometry. All other authors declare no competing interests.

Additional information

Supplementary Information The online version contains supplementary material available at <https://doi.org/10.1038/s41598-022-10231-x>.

Correspondence and requests for materials should be addressed to K.A.

Reprints and permissions information is available at www.nature.com/reprints.

Publisher's note Springer Nature remains neutral with regard to jurisdictional claims in published maps and institutional affiliations.



Open Access This article is licensed under a Creative Commons Attribution 4.0 International License, which permits use, sharing, adaptation, distribution and reproduction in any medium or format, as long as you give appropriate credit to the original author(s) and the source, provide a link to the Creative Commons licence, and indicate if changes were made. The images or other third party material in this article are included in the article's Creative Commons licence, unless indicated otherwise in a credit line to the material. If material is not included in the article's Creative Commons licence and your intended use is not permitted by statutory regulation or exceeds the permitted use, you will need to obtain permission directly from the copyright holder. To view a copy of this licence, visit <http://creativecommons.org/licenses/by/4.0/>.

© The Author(s) 2022